Multi-Objective Optimization of Milling ECSM Process Through PCA-Based GRA

Srivastava, Arpit
Manyawar Kanshiram Government Polytechnic

Sanjeev Kumar Singh Yadav
Harcourt Butler Technical University Kanpur

https://doi.org/10.5109/7160898

出版情報：Evergreen. 10 (4), pp.2230-2236, 2023-12. 九州大学グリーンテクノロジー研究教育センター
バージョン：

Multi-Objective Optimization of Milling ECSM Process Through PCA-Based GRA

Arpit Srivastava[1*], Sanjeev Kumar Singh Yadav[2]
[1]Manyawar Kanshiram Government Polytechnic, Kannauj, India
[2]Harcourt Butler Technical University Kanpur, India

*Author to whom correspondence should be addressed:
E-mail: srivastavaarpit87@gmail.com

(Received August 5, 2023; Revised November 23, 2023; accepted December 11, 2023).

Abstract: Quartz glass has several applications in micro-electrochemical systems (MEMS) and microfluidics systems. Quartz glass micro-channels provide a flexible foundation for various biomedical applications, offering precise fluid control in drug delivery systems, optical navigation, biosensing, and microreactor capabilities. Broad applications of quartz glass create interest in the machining analysis of this material among researchers. Quartz glass machining is challenging due to its highly brittle and non-conductive nature. The electrochemical spark machining (ECSM) process offers efficient and economical machining of quartz material compared to other machining processes, such as Laser beam machining (LBM) and Electron beam machining (EBM). This research performs multi-objective optimization of the milling ECSM process through PCA-based GRA on quartz glass workpiece to achieve a high material removal rate (MRR) with the least surface roughness (S_R). The experiments are designed and performed in Taguchi's L9 orthogonal array. The output machining responses, material removal rate (MRR) and surface roughness (S_R) are optimized through Principal Component Analysis (PCA) based Grey Relational Analysis (GRA). The machining parameters of the milling ECSM process are optimized for maximum MRR and minimum S_R . PCA based GRA technique optimizes machining parameters as voltage 55 V, electrolyte concentration 19 wt.%, tool rotation 600 rpm and duty cycle 0.82.

Keywords: Multi-objective optimization; ECSM; PCA based GRA ;Quartz

1. Introduction

Micro-machining techniques have advanced due to the rapid demand growth for micro products in modern industries. Quartz micro-channels are widely used in the biomedical field, microelectronics mechanical systems , reactors, micro sensors in pressure gauges, micro-balancing, and optics[1-3]. Quartz glass offers excellent physical characteristics such as high hardness, brittleness, and low thermal expansion[4]. These physical properties make quartz glass machining difficult. Wide application but difficulty in machining quartz cause its machining analysis to be crucial. Many advanced manufacturing processes, like laser beam machining, abrasive jet machining, etc., are used to machine the quartz workpiece. Still, all these processes are expensive and offer a low material removal rate[5-7].

Electrochemical spark machining (ECSM) is a hybrid advanced machining process of electric discharge machining (EDM) and electrochemical machining (ECM) processes. ECSM offers machining on conducting and non-conducting materials[8]. ECSM is the best alternative to machine quartz-like workpieces economically and efficiently compared to other machining processes such as LBM, AJM, USM etc. Many investigators investigated different machining issues in ECSM to increase its industrial use. Wuthrich et al.[9] concluded in their study that creating a gas film on the outer surface of the tool electrode is crucial in deciding the effectiveness of the ECSM process. The gas film layer significantly impacts the workpiece surface's quality and the heat-affected zone's width[10].

Many researchers observed the effect of electrolytes on machining performance through ECSM process. Most researchers recommend NaOH, NaCl, $NaNO_3$, HCl, H_2SO_4 as electrolytes in ECSM[11]. Fine graphite powder electrolytes can improve discharge stability, which causes better surface integrity in ECSM[12]. Mallick et al.[13] concluded in their work on ECSM that higher pH electrolytes can improve the material removal rate. Base solution electrolytes produce a better surface finish than acidic solution electrolytes because acidic solution electrolytes have high reactivity, which enhances the surface roughness[14]. Yang et al.[15,16] concluded in their

research work that the smallest hole can be created in ECSM with tungsten carbide tool electrode with minimum tool material losses because tungsten carbide has good thermal stability. Hajian et al.[17] suggested a low feed rate for smaller diameter tool electrodes compared to larger size tool electrodes in milling ECSM because the bending strength of smaller diameter tool electrode is lower, which cause tool bending at an elevated feed rate. Researchers performed experiments with tube tool electrodes. On enhancement in inner diameter, keeping the same outer diameter causes higher material removal rate due to the fact that the smooth and high flow ratio is possible with a bigger inner diameter[18]. Using a magnetic field improves the surface finish during micro-channels formation on glass through ECSM at higher voltage [19]. Magnetic field enhances the gas bubbles repulsion from the tool electrode, resulting in a better surface finish. Different sensors are developed in industries to observe the tool and workpiece surface quality [20,21,22,23].

For recognizing the array of most significant input machining parameters in the ECSM, optimization of input machining parameters is necessary. Several researchers have used the Taguchi method to improve the excellence of output machining parameters[24,25,26,27]. Modern industries have several constraints, like material removal rate, surface finish, economic production cost, etc. So there is a need for multi-optimization techniques for machining process parameters of ECSM. The limitation of the Taguchi method is that this technique can be applied to optimize a single output machining parameter [28]. For Multi optimization, researchers use techniques such as response surface methodology (RSM), principal component analysis(PCA), grey relational analysis(GRA), artificial neural network(ANN) etc. According to researchers, GRA methodology is reliable for multi optimization of micro-machining parameters of the ECSM process[29,30]. In this research work, a hybrid approach of principal component analysis (PCA) based grey relational analysis (GRA) is applied to optimize the multiple outputs of ECSM process, such as MRR and S_R.

2. Problem Formulation

Based on previous research, quartz glass micro-channels are broadly used in sectors like micro-electronics mechanical systems (MEMS), biomedical applications, micro-fluidics, etc. Different researchers investigated and published research on issues in the micro-machining of quartz glass on different machining operations like drilling, milling etc., through ECSM. Research-related multi-optimization of ECSM process parameters in quartz glass micro-machining is limited. This is the driving force behind the current research work, which aims to optimize the response process parameter in ECSM micro-channel fabrication of quartz glass material.

3. ECSM Working Procedure

Fig.1 shows the schematic diagram of the ECSM process. There are two types of electrodes, one tool electrode, which is smaller in size, and the other auxiliary electrode. Both electrodes with workpiece are immersed inside the electrolyte, such as NaOH or KOH. After connecting DC voltage supply, the tool electrode works as a cathode and the auxiliary electrode as an anode. Due to the potential difference between these two electrodes, the electrolysis reaction starts inside the chamber. A growth of hydrogen bubbles forms over the tool electrode's immersed area inside the electrolyte. At critical voltage, these bubbles coalesce and form a gas film at the tool electrode. This gas film behaves like an insulator in between these two electrodes. Due to the barrier of this gas film, an electric spark is created on sufficiently high voltage, results material removal of the workpiece [8].

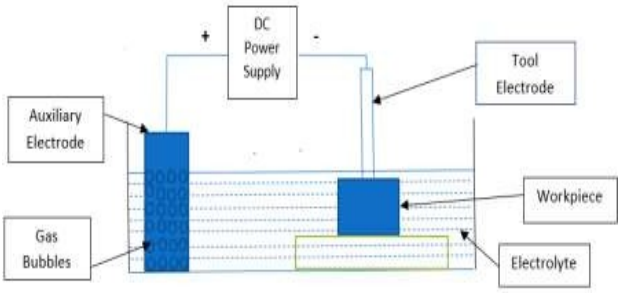

Fig.1: The schematic diagram of the ECSM process

4. Workpiece Material and Machining Setup

Experiments are performed in- housed developed setup of ECSM. There are two units in setup; one is for machining, and the other is for supplying power to the machine. Fig. 2 shows the ECSM setup. An acrylic machining chamber is used for the electrolysis mechanism in the machining unit. Three-axis motion was made possible through 12 V DC three-stepper motors. The system is connected to a computer, and CNC USB controller software controls the axial movement in setup. The diameter of the tool electrode and auxiliary electrodes are 370 µm and 2 mm, respectively. In this study, a 370 µm copper tool is selected to fabricate micro-channels because a below 370 µm diameter copper tool is not stiff enough to stand on the machining zone without tool electrode bending. The bigger size of the auxiliary electrode aids in distributing the more significant amount of ions towards the tool electrode. These ions quickly cover the smaller size of the tool electrode in the form of bubbles and film. Both electrodes are made of copper to minimize electrode wear. A separate DC motor is used to provide the rotary motion of the tool electrode. All experimental observations maintained the inter-electrode distance between the tool and auxiliary electrodes at up to 50mm. A quartz glass plate of size (50mm × 25mm × 2mm) is used as a workpiece on which micro-channels are formed. NaOH is used as an electrolyte for this research

work. Tool travel speed is 2.5 mm/min within two minutes of machining time in each experiment. This setup's power supply unit can produce DC pulse voltage. A range of DC voltage from 45 V to 55 V is selected for performing experimental work. The characteristics of the quartz glass workpiece are shown in Table 1.

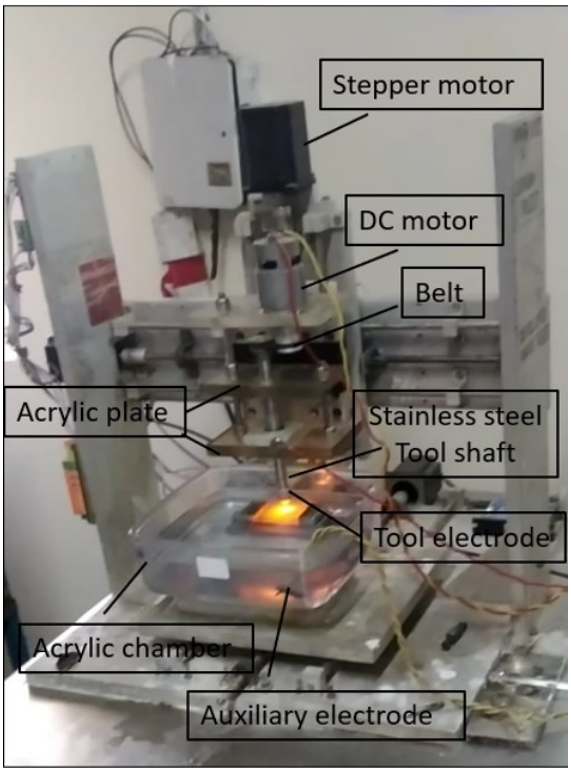

Fig.2: Machine unit of ECSM setup during the machining process

Table 1. Essential Properties of the quartz glass workpiece

Young's modulus	108 GPa
Density	2.2 gm/cm^3
Softening Temperature	1700^0C (Approximate)
Thermal Conductivity	1.38 *W/mk*

5. Machining Method and Environments

This research aims to determine the set of optimum input machining parameters of ECSM for multi-objective optimization of output machining parameters. The experiments are designed and performed in Taguchi's L9 orthogonal array. DC voltage, electrolyte concentration(wt.%), tool rotation and duty cycle are input machining process parameters. Material removal rate and surface roughness are output machining process parameters for studying the quality of the machining operation. The weight of the workpiece before and after the machining is measured to determine MRR. Denver SI 234 weight machine with an accuracy of 0.01 mg is used to measure the workpiece's weight. Mitutoyo Surftest SV-2100 measures the surface roughness of micro-channels. A digital laser tachometer measures tool rotation during the experiment. The computed output machining parameters are examined by considering the S/N ratio "higher- the- better" for material removal rate and " smaller-the-better" for surface roughness. The input machining parameters levels and factors for this experimental work are shown in Tables 2 and 3. The scope of input machining parameters is decided on the results of pilot experiments and covered literature review. Table 4 shows the experimental plan.

Table 2 Constant Machining Parameters

Constant Machining Parameters	
Tool electrode and auxiliary electrode material	Copper
Tool electrode size	370 µm diameter
Workpiece	Quartz plate
Electrolyte	NaOH
Machining Time	2 min
Tool travel rate	2.5*mm/min*
Electrolyte level	Up to 1 mm above the quartz plate

Table 3. Experimental Variable Parameters

Variable Parameters	
Voltage	*45V*,50*V*,55*V*
Duty Cycle	0.75, 0.82,0.89
Tool Rotation	400rpm,600rpm,800rpm
Electrolyte Concentration	19*wt%,24wt%,29wt%*

6. Results and Discussions

6.1 Multi-Objective Optimization through PCA-based GRA

These are the steps for Multi-objective optimization using PCA based GRA technique is used in this research work:

Step 1: The computed output machining parameters are examined by considering the S/N ratio "higher- the- better" for material removal rate according to eq.1

$$\eta_{ij} = -10log\left[\frac{1}{n}\sum_{i=1}^{n}\bar{z}_i^{-2}\right] \quad (1)$$

Table 4. Experimental parameters design

Experiment No.	Voltage	Electrolyte Concentration	Duty Cycle	Tool Rotation	MRR	S_R
	(V)	*(wt%)*		*(RPM)*	*(mg/min)*	*(μm)*
1	45	19	0.75	400	0.45	1.9
2	45	24	0.82	600	0.60	3.2
3	45	29	0.89	800	0.35	4.319
4	50	19	0.75	600	0.90	1.670
5	50	24	0.82	800	0.65	3.60
6	50	29	0.89	400	0.65	3.42
7	55	19	0.82	600	1.10	1.5
8	55	24	0.75	400	0.80	3
9	55	29	0.89	800	0.60	2.1

Step 2: The computed output machining parameters are examined by considering the S/N ratio " smaller-the-better" for surface roughness of micro-channels on workpiece according to eq.2

$$\eta_{ij} = -10log\left[\frac{1}{n}\sum_{i=1}^{n}\bar{z}_i^2\right] \quad (2)$$

where η_{ij} = Single-to-noise ratio corresponding to i number experiment and j number response.

n = Number of replications of the individual experiment.

$\bar{z}_i$ = average value of z_i observations.

Step 3: Principal component scores (P_{cs}) can be measured by Eq.3

$$P_{cs_{il}} = a_{l1}\eta_{i1} + a_{l2}\eta_{i2} + a_{l3}\eta_{i3} + \ldots\ldots + a_{lj}\eta_{ij} \quad (3)$$

Step 4: To get optimum results, there is a need for the highest value of P_{cs}. For this reason, the normalization of P_{cs} data is performed through eq.4

$$y_{il} = \frac{P_{cs_{il}} - P_{cs_l}^{min}}{P_{cs_l}^{max} - P_{cs_l}^{min}} \quad (4)$$

Where

$P_{cs_{il}}$ = normalized P_{cs} for i^{th} experiment and l^{th} reponse(l = j).

Step 5: Calculation of Grey relational coefficients (GRC) is calculated through eq.5

$$€_{il} = \frac{\boldsymbol{\beta}^{max} + \Psi\boldsymbol{\beta}^{min}}{\boldsymbol{\beta}_{il} - \Psi\boldsymbol{\beta}^{min}} \quad (5)$$

Here $\boldsymbol{\beta}_{il}$ = difference in values of X_{il} and reference order X_O. If X_O=1, then

$$\beta_{il} = X_O - X_{il} = 1 - X_{il} \quad (6)$$

Here Ψ is called the coefficient of distinguishing in the mid of zero and one. It is used to increase the variance significance. $\Psi = 0.5$ for the global maximum $\boldsymbol{\beta}^{max}$ and global minimum $\boldsymbol{\beta}^{min}$.

Step-6: Overall quality performance index (OQPI) is measured through the equation:

$$OQPI_i = \frac{1}{N}\sum_{i=1}^{n}\sum_{l=1}^{j} P_l €_{il} \quad (7)$$

Here P_l is the percentage of an individual output variable, and N represents the quantity output variables and $\sum_{l=1}^{j} P_l = 1$.

Step-7: The parameters with maximum OQPI are considered optimal parameters getting through the main effects plot. For MRR and S_R, the S/N ratio consider higher-the-better and smaller-the-better, respectively. Table 5 shows the principal components in the form of a correlation matrix with eigenvalues.

Equation 3 calculates the principal components scores (P_{cs}) for MRR and S_R. Normalization of these principal components scores (P_{cs}) are performed through equation 4. Equation 5 calculates grey relational coefficients with a value of the coefficient of distinguishing Ψ as 0.5. Ultimately, the overall quality performance index (OQPI) is decided through equation 7. Table 6 shows the signal to noise ratio (S/N ratio), principal components scores ($P_{cs_{il}}$), grey relational coefficients (GRC) and overall quality performance index (OQPI).

Table 5. Principal components, eigenvalues analysis as a correlation matrix

Response Variables	Eigen Vectors		Eigen Value	Proportion
	PC1	PC2		
S/N-MRR	-0.707	-0.707	1.6035	0.802
S/N-S_R	0.707	-0.707	0.3965	0.198

Table 6. Calculated S/N ratio, $P_{cs_{il}}$, GRC and OQPI

Experiment No.	S/N-MRR	S/N- S_R	$P_{cs_{i1}}$	$P_{cs_{i2}}$	GRC		OQPI
					$€_{i1}$	$€_{i2}$	γ
1	-6.936	-5.575	-8.845	0.962	0.466	1.000	0.267
2	-4.437	-10.103	-10.280	-4.006	0.429	0.396	0.212
3	-9.119	-12.708	-15.431	-2.537	0.333	0.483	0.176
4	-0.915	-4.454	-3.796	-2.502	0.670	0.485	0.323
5	-3.742	-11.126	-10.512	-5.221	0.423	0.345	0.207
6	-3.742	-10.681	-10.197	-4.906	0.431	0.357	0.211
7	0.828	-3.522	-1.905	-3.075	0.802	0.447	0.378
8	-1.938	-9.542	-8.117	-5.376	0.487	0.340	0.234
9	-4.437	-6.444	-7.693	-1.419	0.501	0.578	0.255

6.2 Optimized machining parameters

The optimized set of input parameters conditions is defined by OQPI curve as shown in Fig.3. Each optimal input machining parameter is decided to correspond to the peak value of OQPI. The OQPI curve suggests optimum parameters are voltage 55 V, electrolyte concentration 19 *wt.%,* tool rotation 600 rpm and duty cycle 0.82. Minitab is the software used for this optimization process, and three times experimental run were performed for each combination of parameters.

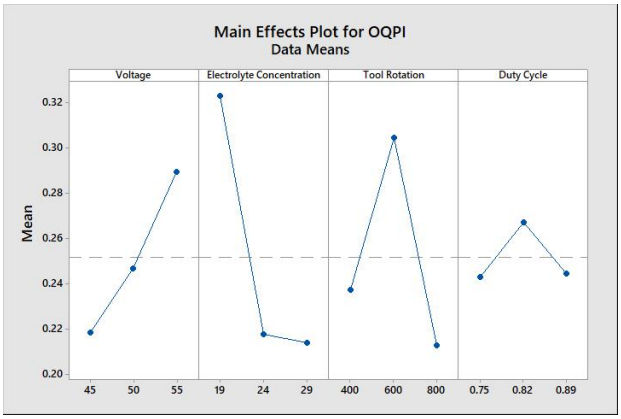

Fig.3: OQPI Main Effect Plot

6.3 Confirmation Experiment Result

Confirmation tests at the optimal parameter setting are carried out to validate the optimal machining parameter setting derived using the PCA based GRA technique. Table 7 shows the results of the confirmation experiment. The confirmation experiment is executed at optimal input machining parameters. It is reported that OQPI calculated from the confirmation experiment result has a 6.61% error from the predicted OQPI. This least error value shows that results are validated on optimal input machining conditions.

Table 7. Confirmation Experiment Result

S.No.	Voltage	Electrolyte Concentration	Tool Rotation	Duty Cycle	MRR	S_R
	(V)	(*%wt*)	*(rpm)*		*(mg/min)*	*(µm)*
1.	55	19	600	0.82	1.12	1.7

7. Conclusion

In this research work, the milling ECSM process performance on quartz glass is observed in terms of MRR and S_R . This process performance is investigated through the multi-objective optimization of the milling ECSM process with PCA-based GRA approach for deciding the optimized machining process parameters. The combination of MRR as maximum and S_R as minimum is considered to determine the optimized range of machining process parameters. The conclusions of this research work can be specified as:

- It is reported that the OQPI calculated from the confirmation experiment result has a 6.61% error from the predicted OQPI at the optimal parameter settings.
- The optimum parameters in the milling ECSM process are determined as voltage 55 V, electrolyte concentration 19 *wt.%,* tool rotation 600 rpm and duty

cycle 0.82.

- In this research work, output machining parameters MRR and S_R are measured by input machining parameters applied voltage, electrolyte concentration, tool rotation and duty cycle.
- The PCA-based GRA technique is appropriate for the execution of multi-objective optimization. It creates a set of optimized machining process parameters to enhance the quality of ECSM process output during the machining of quartz workpieces.

Nomenclature

ECSM	Electrochemical Spark Machining
PCA	Principal Component Analysis
GRA	Grey Relational Analysis
MRR	Material Removal Rate
S_R	Surface Roughness
S/N ratio	Signal to noise ratio
OQPI	Overall Quality Performance Index
GRC	Grey Relational Coefficients
P_{cs}	Principal component scores

References

1) M. Sandison, M. Zagnoni , M. Abu-hantash , H. Morgan, " Micromachined glass apertures for artificial lipid bilayer formation in a microfluidic system", J Micromech Microeng ,(17) 189–196 (2007). https://doi.org/10.1088/0960-1317/17/7/S172.
2) H. San , H. Zhang , Q. Zhang , C. YuY , "Silicon – glass-based single piezoresistive pressure sensors for harsh environment", J Micromech Microeng, (23) 20-75 (2013). https://doi.org/10.1088/0960- 1317/23/7/075020
3) O. Isabella, F. Moll , J Krc , M Zeman, "Modulated surface textures using zinc-oxide films for solar cells applications", Phys Status Solidi Appl Mater Sci,(207) 642–646 (2010). https://doi.org/10. 1002/pssa.200982828
4) N. Rattan , R. Mulik, "Experimental set up to improve machining performance of silicon dioxide (quartz) in magnetic field assisted TW-ECSM process", Silicon, 10(6) 2783–2791 (2018). https://doi.org/10.1007/s12633-018-9818-z
5) H. Feng , D. Xiang , B. Wu , B. Zhao, "Ultrasonic vibration assisted grinding of blind holes and internal threads in cemented carbides", Int J Adv Manuf Technol, 104(1–4) 1357–1367 (2019). https:// doi.org/10.1007/s00170-019-04024-2
6) A. Belyaev , O. Polupan , W. Dallas , S. Ostapenko , D. Hess , J. Wohlgemuth), "Crack detection and analyses using resonance ultrasonic vibrations in full-size crystalline silicon wafers",Appl Phys Lett 88(11) 111-121(2006). https://doi.org/10.1109/WCPEC.2006.279606
7) Y. Tang , J. Fuh , H. Loh , Y. Wong , Y. Lim, "Laser dicing of silicon wafer", Surf Rev Lett 15(01n02) 153–159(2008). https://doi.org/10.1142/S0218625X08011147
8) A. Srivastava , S. Yadav, "Machining issues on electrochemical spark machining—a review. Materials Today", Proceedings, (Jan 1;26), 2853-2861 (2020). https://doi.org/10.1016/j.matpr.2020.02.593
9) R. Wuthrich , L. Hof , "The gas film in spark assisted chemical engraving SACE—a key element for micro-machining applications", Int J Mach Tools Manuf, (46) 828–835 (2005). https://doi.org/10. 1016/jijmachtools200507029
10) M. Sundaram ,Y. Chen , K. Rajurkar, "Pulse electrochemical discharge machining of glass-fiber epoxy reinforced composite" ,CIRP Ann 68(1) 169–172 (2019). https://doi.org/10.1016/jcirp201904113
11) B. Jiang, S. Lan, K. Wilt, J. Ni, "Modeling and experimental investigation of gas film in micro-electrochemical discharge machining process", *International Journal of Machine Tools and Manufacture*, (*90)* 8-15 (2015). https://doi.org/10.1016/j.ijmachtools.2014.11.006
12) R. Wüthrich, and V. Fascio, "Machining of non-conducting materials using electrochemical discharge phenomenon—an overview",*International Journal of Machine Tools and Manufacture*, *45*(9) 1095-1108 (2005). https://doi.org/10.1016/j.ijmachtools.2004.11.011
13) B. Mallick, M. Ali, B. Sarkar, B. Doloi, B. Bhattacharyya, "Parametric analysis of electrochemical discharge micro-machining process during profile generation on glass", Proceeding of International Conference on All India Manufacturing Technology, Design and Research Conference (AIMTDR), IIT Guwahati, India (26) 5401–5406 (2014).
14) Kulkarni, "Electrochemical Spark Micromachining Process, Micromachining Techniques for Fabrication of Micro and Nano Structures", Dr. MojtabaKahrizi (Ed.), ISBN: 978-953-307-906-6, (2012).
15) C. Yang, C. Cheng, C. Mai, C. Wang, J. Hang, B. Yan, "Effect of surface roughness of tool electrode materials in ECDM process", Int. J. Mach. Tool Manuf. (50) 1088–1096 (2010). http://dx.doi.org/10.1016/j.ijmachtools.2010.08.006
16) C. Yang, K. Wu, J. Hung, S. Lee, J. Lin, B. Yan, " Enhancement of ECDM Efficiency and accuracy by Spherical tool Electrode", Int. J. Mach. Tools Manuf. (51) 528–535 (2011). https://doi.org/10.1016/j.ijmachtools.2011.03.001
17) M. Hajian, M. Razfar, A. Etefagh, "Experimental study of tool bending force and feed rate in ECDM

Milling", Int. J. Adv. Manuf. Technol. (91) 1677–1687 (2017). https://doi.org/10.1007/s00170-016-9860-1

18) Y. Zhang, Z. Xu, Y. Zhu, D. Zhu, "Effect of tube electrode inner structure on Machining performance in tube electrode High-speed Electrochemical Discharge drilling", J. Mater. Process. Technol. 231 (2016) 38–49. https://doi.org/10.1016/j.freeradbiomed.2016.05.017
19) M. Hajian, M. Razfar, the S. Movahed, "An Experimental study on the effect of Magnetic field orientations and Electrolyte concentrations on ECDM milling performance of glass", Precision Eng. (45) 322–331 (2016). https://doi.org/10.1016/j.precisioneng.2016.03.009
20) T. Dief, and S. Yoshida, "System identification for quad-rotor parameters using neural network," EVERGREEN Joint Journal of Novel Carbon Resource Sciences & Green Asia Strategy, 3(1), 6–11 (2016). https://doi.org/10.5109/1657380
21) M. Berawi, S. Siahaan, P. Miraj, and P. Leviakangas, "Determining the prioritized victim of earthquake disaster using fuzzy logic and decision tree approach," EVERGREEN Joint Journal of Novel Carbon Resource Sciences & Green Asia Strategy, 7(2), 246–252 (2020). https://doi.org/10.5109/4055227
22) S. Dwivedi, N.Maurya, and M. Maurya, "Assessment of Hardness on AA 2014/Eggshell composite Produced Via Electromagnetic Stir Casting Method", EVERGREEN Joint Journal of Novel Carbon Resource Sciences & Green Asia Strategy, 6(4), 285-294 (2019). https://doi.org/10.5109/2547354
23) M. Maurya, N. Maurya, and V. Bajpai, "Effect of SiC Reinforced Particle Parameters in the Development of Aluminium Based Metal Matrix Composite", EVERGREEN Joint Journal of Novel Carbon Resource Sciences & Green Asia Strategy, 6(3), 200-206 (2019). https://doi.org/10.5109/2349295
24) T. Muthuramalingam, S. Vasanth , P. Vinothkumar , T. Geethapriyan , M. Rabik, "Multi criteria decision making of abrasive flow oriented process parameters in abrasive water jet machining using Taguchi–DEAR methodology",Silicon 10(5) 2015–2021 (2019). https://doi.org/10.1007/s12633-020-00573-4
25) P. Antil , S. Singh ,P. Singh, "Taguchi's methodology based parametric analysis of material removal rate during ECDM of PMCs", Procedia Manuf (26) 469–473 (2019). 10.1016/j.promfg.2018.07.055
26) P. Gupta, B. Singh, Y. Shrivastava, "Theoretical and Experimental Prediction of Optimal Process Variables for Enhanced Metal Removal Rate During Turning on CNC lathe" ", EVERGREEN Joint Journal of Novel Carbon Resource Sciences & Green Asia Strategy, 10(2), 1127-1132 (2023). https://doi.org/10.5109/6793673
27) A. Chandra, A. Yadav, S. Singh, P. Arora, "Optimisation of Machining Parameters for CNC Milling of Fibre Reinforced Polymers" 10(2), 765-773 (2023).
28) P. Ross, "Taguchi Techniques for Quality Engineering, second ed.", Tata McGraw-Hill publishing company limited, New Delhi, (2005).
29) M. Goud , A.Sharma , "On performance studies during micromachining of quartz glass using electrochemical discharge machining", J Mech Sci Technol (31) 1365–1372 (2017). https://doi.org/10. 1007/s12206-017-0236
30) P. Antil , "Modelling and multi-objective optimization during ECDM of silicon carbide reinforced epoxy composites", Silicon, 10(6) 1–14 (2019). https://doi.org/10.1007/s12633-019-00122-8